Low-temperature resistivity of bulk copper-aluminum alloys

C. Macchioni, J. A. Rayne, and C. L. Bauer
Center for Joining of Materials, Carnegie-Mellon University, Pittsburgh, Pennsylvania 15213
(Received 30 September 1981)

Resistivity measurements from 4.2 to 300 K have been made on a series of well-characterized bulk samples covering the entire copper-aluminum phase diagram. For the cubic terminal solid solutions the values of $d\rho/dc$ can be well described by a simple phase-shift analysis taking into account the different lattice parameters of copper and aluminum. The resistivity of the γ_2 phase is strongly dependent on composition as a result of the rapid decrease in Fermi-surface area with electron concentration. Results for the other phases are discussed and compared to recently reported thin-film resistivity data.

I. INTRODUCTION

Apart from its intrinsic physical interest, the copper-aluminum system is of considerable technological importance. Copper and aluminum films play a crucial role in modern integrated circuits, the reliability of which are significantly affected by electromigration effects and interfacial reactions in the films. The latter have recently been studied by contact resistance measurements in copper-aluminum couples.[1] During the course of this research, the need for reliable resistivity data in thin-film and bulk samples of alloy phases in the copper-aluminum system became apparent.

Thin-film data[2] have recently been obtained for the θ phase ($CuAl_2$) and γ_2 phase (Cu_9Al_4). In the present paper we report resistivity measurements from 4.2 to 300 K on a series of well-characterized bulk samples covering the entire copper-aluminum phase diagram. For the cubic terminal solid solutions, the resistivity can be well described by a simple phase-shift analysis taking into account the difference in lattice parameters of copper and aluminum. The resistivity of the γ_2 phase is strongly dependent on composition, as a result of the rapid decrease in Fermi-surface area with electron concentration. Results for the other phases are discussed in relation to the virtual crystal model for a simple binary alloy and are compared with thin-film data.

II. EXPERIMENT

The phase diagram for the copper-aluminum system is quite complex. Reference to Table I shows that, in addition to the cubic terminal solid solutions, there are five intermediate phases. Both the γ_2 and δ are complex cubic structures, the former having the approximate composition Cu_9Al_4 with a stability range extending from 31 to 37 at.%. There is some disagreement about the structure of the δ phase,[3] which occurs over a relatively narrow range near 40 at.% corresponding to the composition Cu_3Al_2. The remaining phases ζ_2, η_2, and θ all have narrow stability ranges, corresponding to the compositions Cu_4Al_3, CuAl, and $CuAl_2$, respectively. Some doubt also exists about the structure of the ζ_2 phase.[3]

Samples of the alloy phases covering the entire phase diagram were prepared by induction melting 99.999 + % pure copper and aluminum in recrystallized alumina crucibles under an argon atmosphere. The resulting ingots were then annealed in argon, close to the maximum temperature consistent with stability as determined from the relevant part of the phase diagram. Table II summarizes x-ray data taken from powder samples obtained from the heat-treated ingots. As can be seen, there is good agreeement with the observed lattice parameters and accepted values.[3] Resistivity samples, in the form of rectangular parallelepipeds approximately 2 cm long and 1.5 mm by 1.5 mm cross section, were cut from the ingots by spark erosion. The measurements were made by a four-probe method using an automatic system interfaced to a PDP-11 minicomputer. Details of this apparatus have been described in a previous paper.[1]

III. RESULTS

Figure 1 shows the variation of room-temperature resistivity as a function of composi-

TABLE I. Properties of phases in copper-aluminum system.

Phase	Nominal composition	Lattice	Space group
α	(Cu)	Cubic	$Fm3m$
γ_2	Cu_9Al_4	Cubic	$P\bar{4}3m$
δ	Cu_3Al_2	Cubic	$I\bar{4}3m$
ζ_2	Cu_4Al_3	Monoclinic	
η_2	CuAl	Monoclinic	$C2/m$
θ	$CuAl_2$	Tetragonal	$I4/mcm$
β	(Al)	Cubic	$Fm3m$

tion in the copper-aluminum system. At low solute concentrations, the results for the primary solid solutions are in good agreement with previous data[4,5] given by the dashed lines. The values of $d\rho/dc$ for *Cu*Al and *Al*Cu are 1.30 ± 0.10 and 0.95 ± 0.10 $\mu\Omega$ cm per atomic percent, respectively. At high concentrations in *Cu*Al there is appreciable deviation from linearity due to solute interaction effects, as in the case of other primary solid solutions such as *Cu*Zn and *Cu*Ge.[6,7]

The most salient feature of the results for the intermediate phases is the very high resistivity for the γ_2 and δ phases and the strong composition dependence in the former. As is demonstrated later, this behavior is essentially an electronic effect associated with the γ-brass band structure. The resistivity of the electron compounds corresponding to the ζ_2, η_2, and θ phases is similar to that observed in polyvalent pure metals. There is reasonable agreement between the present data for bulk samples and the data for thin films prepared by electron beam evaporation.[8]

Figures 2 and 3 show the temperature dependence of the resistivity for the primary solid solutions *Cu*Al and *Al*Cu, respectively. For dilute alloys it can be seen that Matthiesen's rule is obeyed, the graphs being essentially parallel to those for pure copper and aluminum. For more concentrat-

TABLE II. Summary of measured properties of copper-aluminum alloys.

Phase[a]	Composition (at. %)	ρ_{295} ($\mu\Omega$ cm)	$\rho_{4.2}$ ($\mu\Omega$ cm)	RRR[b]	TCR[c] ($10^{-3}K^{-1}$)	Lattice parameter (Å) measured	literature[d]
α(Cu)	2.3	4.79±0.18	2.85±0.11	1.68±0.09	3.98±0.18	3.616±0.014	3.615(0)
	8.9	8.97±0.37	6.73±0.27	1.33±0.08	3.82±0.16	3.630±0.017	
	16.5	11.04±0.39	7.97±0.28	1.39±0.07	3.53±0.17	3.658±0.012	3.659(17.26)
$\gamma_2(Cu_9Al_4)$	31	17.27±0.85	8.30±0.41	2.08±0.15	3.64±0.02	8.693±0.009	8.709(31.76)
	34.1	18.47±0.74	8.76±0.35	2.11±0.12	4.14±0.06	8.702±0.006	8.716±(33.32)
	36.8	25.94±1.27	17.28±0.85	1.50±0.10	3.71±0.03	8.690±0.007	
$\delta(Cu_3Al_2)$	38.8	28.83±1.41	20.46±1.00	1.40±0.10	3.77±0.04	8.679±.012	
$\zeta_2(Cu_4Al_3)$	44.0	12.67±0.60	5.13±0.23	2.47±0.16	3.60±0.07		
η_2(CuAl)	49.0	8.67±0.42	2.96±0.15	2.93±0.21	4.06±0.05	12.045±0.026	12.066
$\theta(CuAl_2)$	66.6	7.64±0.23	0.86±0.04	8.88±0.17	4.09±0.11	6.066±0.016 ($c=4.874\pm0.042$)	6.066(67.6) ($c=4.874$)
β(Al)	98.26	3.95±0.15	0.999±0.04	3.95±0.22	4.17±0.08	4.037±0.006	4.042(98.38)
	99.14	3.12±0.10	0.44±0.04	7.12±0.69	4.11±0.30	4.043±0.006	4.045(99.20)

[a]Approximate chemical composition given in parentheses.
[b]RRR is residual resistance ratio $\rho_{295}/\rho_{4.2}$
[c]TCR is temperature coefficient of resistance $[1/(\rho_{295}-\rho_{4.2})]d\rho/dT$ evaluated at 295 K.
[d]Lattice parameters from Ref. 3. Values in parentheses are compositions corresponding to quoted lattice parameters.

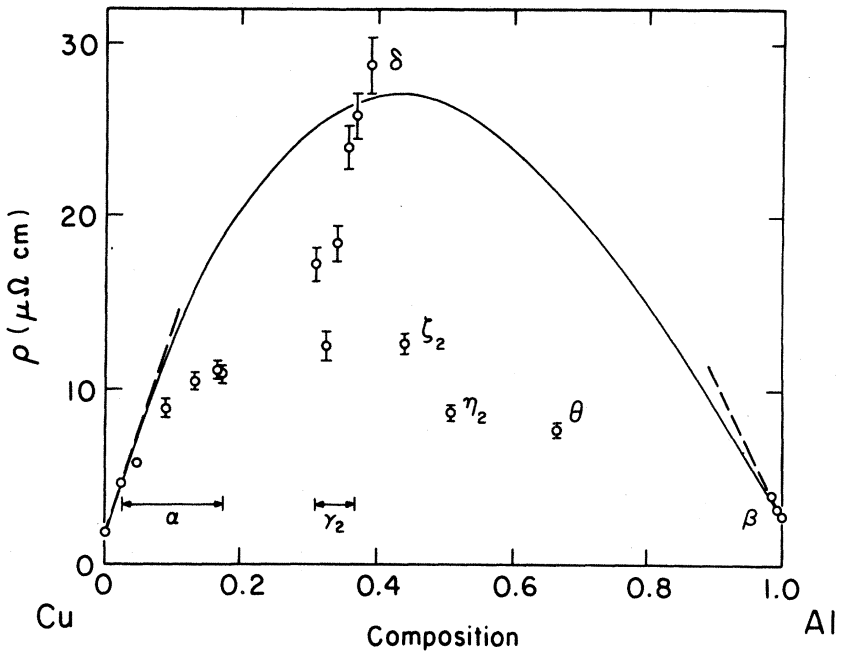

FIG. 1. Variation of room-temperature resistivity as a function of composition in copper-aluminum alloys. Dashed lines give limiting slopes for primary solid solutions determined by previous workers. Solid curve is concentration dependence predicted by virtual-crystal model discussed in text.

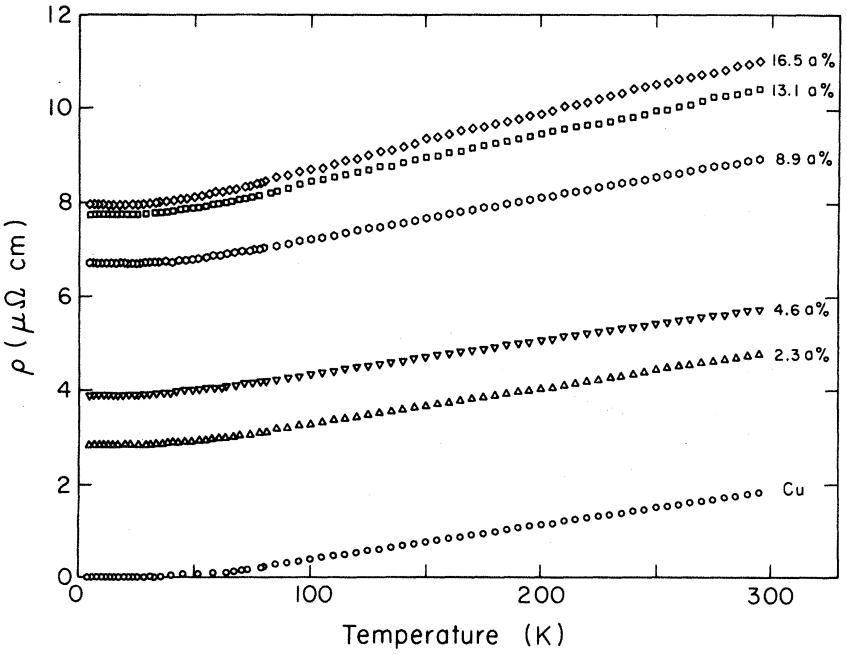

FIG. 2. Temperature dependence of resistivity for primary solid solution *Cu*Al. Concentration of aluminum in atomic percent is shown beside data for each alloy specimen.

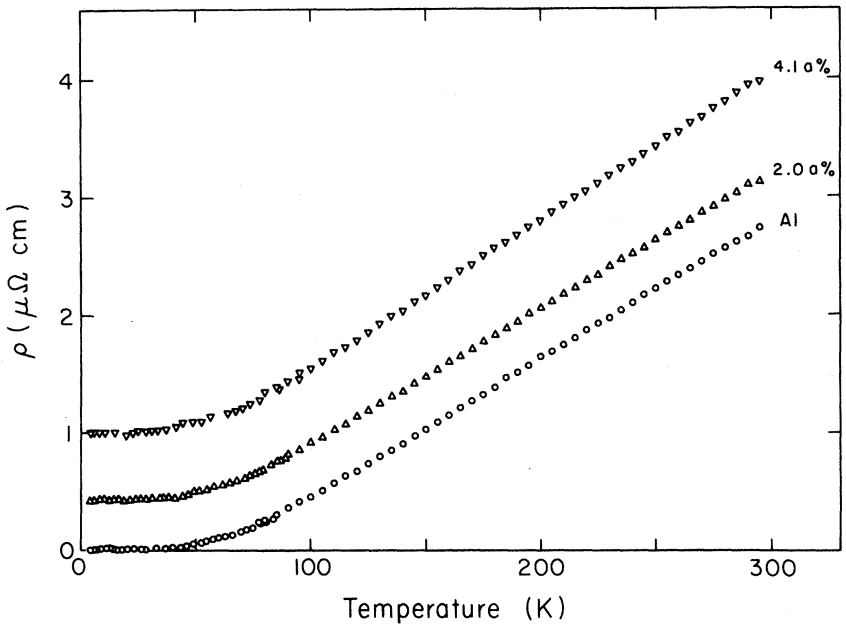

FIG. 3. Temperature dependence of resistivity for primary solid solution *Al*Cu. Concentration of copper in atomic percent is shown beside data for each alloy specimen.

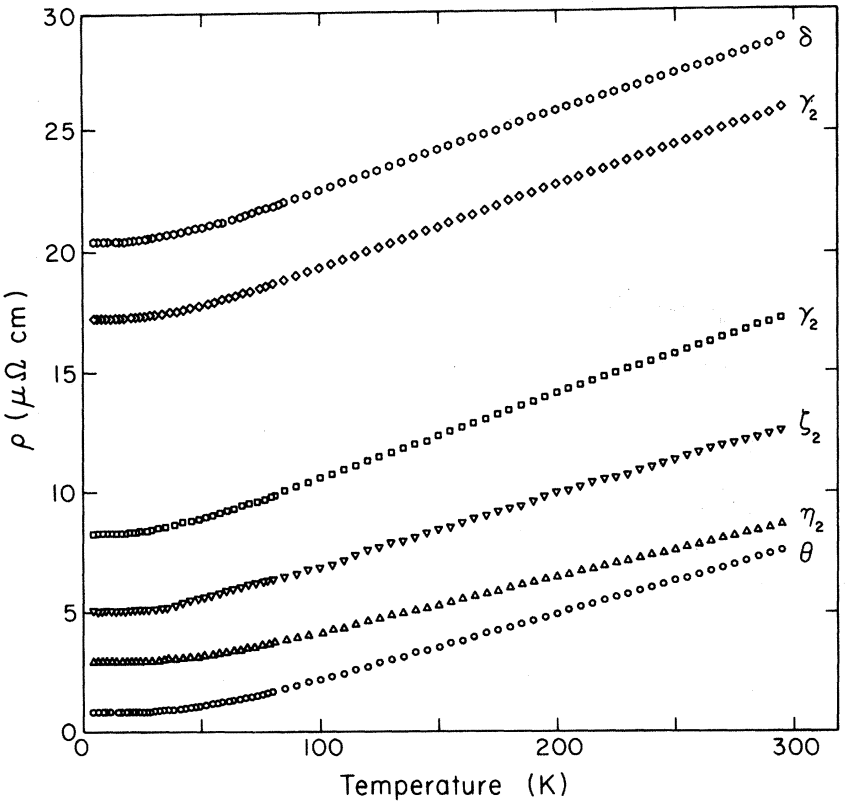

FIG. 4. Temperature dependence of resistivity for intermediate phases in copper-aluminum system. Data for γ_2 phase corresponds to 37 at. % Al (upper curve) and 31 at. % Al (lower curve), respectively.

ed *Cu*Al alloys, deviations from this behavior are clearly visible, the temperature coefficient of resistance decreasing from 3.8×10^{-3} K^{-1} for pure copper to 3.5×10^{-3} K^{-1} for the 16 at. % alloy. The initial values of $d\rho/dc$ at 4.2 K are essentially identical to those obtained at 300 K.

The temperature dependence of the resistivity of the intermediate phases in the copper-aluminum system is shown in Fig. 4. It can be seen that the resistance behavior of the θ phase is similar to that for a pure metal, the residual resistivity ratio (RRR) being approximately 8 to 1. Clearly this phase is an ordered intermetallic compound with the exact composition $CuAl_2$. Neither the η_2 nor ζ_2 phases has such high values of RRR, presumably because at equilibrium they deviate from stoichiometry. In the case of the γ_2 and δ phases, the RRR is close to unity, corresponding to a disordered alloy. Table II summarizes the resistivity data at both 4.2 and 300 K.

IV. DISCUSSION

In considering these results, let us first apply a simple phase-shift analysis to the behavior of the terminal solid solutions. For a simple fcc alloy containing a concentration n_i of impurities, the resistivity ρ is given by the equation[9]

$$\rho=\frac{n_i}{n}\frac{4\pi\hbar}{e^2k_F}\sum_{l=0}^{\infty}(l+1)\sin^2(\eta_l-\eta_{l+1})\ . \tag{1}$$

Here n is the conduction electron density and k_F is the Fermi wave vector given by

$$k_F=\frac{2\pi}{a}\left[\frac{3v}{2\pi}\right]^{1/3}\ , \tag{2}$$

where a,v are the relevant lattice parameter and valence of the solvent. The phase shifts η_l obey the Friedel sum rule

$$Z=\frac{2}{\pi}\sum_{l=0}^{\infty}(2l+1)\eta_l\ , \tag{3}$$

where Z is the relative valence of solute and solvent. In the present case $Z=\pm2$, so that if only a single phase shift is dominant, the lowest value of l giving a nonzero value of $d\rho/dc$ is unity. From Eqs. (1) and (2) we then obtain with $a_{Cu}=3.615$ Å and $a_{Al}=4.060$ Å,

$$\frac{\left[\frac{d\rho}{dc}\right]_{CuAl}}{\left[\frac{d\rho}{dc}\right]_{AlCu}}=\left[\frac{v_{Al}}{v_{Cu}}\right]^{4/3}\left[\frac{a_{Cu}}{a_{Al}}\right]^4=2.72\ , \tag{4}$$

which is much greater than the observed ratio of 1.4. Clearly, additional partial waves must be invoked to obtain agreement with experiment. Now p-wave scattering is expected to be dominant for copper alloys,[10] while s-wave scattering is important in aluminum alloys. Hence, it is more reasonable to include terms corresponding to $l=0,1$ in evaluating Eq. (1) for the case of *Al*Cu and to retain only the $l=1$ term for *Cu*Al. We then have

$$\frac{\left[\frac{d\rho}{dc}\right]_{CuAl}}{\left[\frac{d\rho}{dc}\right]_{AlCu}}=2.72\frac{2\sin^2\frac{\pi}{3}}{\sin^2(\eta_0-\eta_1)+2\sin^2\eta_1}\ , \tag{5}$$

where the phase shifts η_0,η_1 for *Al*Cu are related by the Friedel sum rule with $Z=-2$. The resulting ratio has a minimum value of approximately 1.5, which is close to the experimental figure. However, it is evident that the corresponding value of $\eta_1=-1.2$ is not to be taken too seriously. Rather, this analysis simply shows that the larger value of $d\rho/dc$ in *Cu*Al compared with *Al*Cu is the result of the increased importance of p-wave scattering in the former case. This conclusion is consistent with de Haas–van Alphen (dHvA) studies on dilute noble-metal alloys,[11] which in fact show that d-wave scattering is also significant in such systems.

of the resistivity in the copper-aluminum system with the predictions of a virtual-crystal model, considering only the effects of change in composition and neglecting any changes in the crystal structure. A simple calculation shows that the impurity ρ resistivity for the alloy A_xB_{1-x} is given by

$$\rho=x(1-x)[\alpha_1+(\alpha_2-\alpha_1)x]\,|M|^2\ , \tag{6}$$

where M is the matrix element of the difference potential (V_A-V_B) and α_1,α_2 take into account the difference in valence between the constituents A,B. For the simple case where A,B are homovalent, α_1 is equal to α_2 and Eq. (6) reduces to the usual

Nordheim relation.[12] The full curve in Fig. 1 is calculated from Eq. (6), where the values of α_1 and α_2 have been adjusted to fit the initial slopes of the primary solid solutions. Evidently, the discrepancy between the observed and predicted behavior for the ζ_2, η_2, and θ phases is connected with the fact that these are ordered electron compounds and not disordered systems as implied by the model. In this connection, it is noteworthy that the data for both the γ_2 and δ phases do fit the curve reasonably well, thereby lending further support to the hypothesis that they are disordered systems.

As noted previously the resistivity of the γ_2 phase depends very strongly on composition, a pronounced minimum being obseved at approximately 32 at. % aluminum. This behavior is believed to be associated with the electronic structure of γ-brass alloys, which can be understood in terms of the Jones zone formed by the (330) and (411) planes of the reciprocal lattice for a simple cubic structure.[13] All these planes are at the same distance from the zone center, so that if the Fermi surface is spherical, it simultaneously contacts all 36 zone faces as the electron concentration increases. Subsequently, the Fermi-surface area and density of states at the Fermi energy will initially decrease quite rapidly.

Specific-heat measurements[14] have shown that this decrease in fact occurs in the case of γ-brass alloys and that the behavior is quite well described by a simple model, in which the Fermi surface is a sphere truncated by the planes comprising the Jones zone. Now the conductivity of a metal is given by the usual relation

$$\sigma = \frac{e^2}{12\pi^3\hbar}\langle \tau v \rangle S_F \,, \tag{7}$$

where S_F is the Fermi-surface area and $\langle \tau v \rangle$ is the average over the Fermi surface of the product of the relaxation time τ and carrier velocity v. The present results suggest that the observed increase in ρ beyond 32 at. % aluminum is due to the rapid reduction in S_F with increasing concentration. Since the carrier velocity v is a slowly varying function of energy, the sharp initial decrease in the observed resistivity must be ascribed to a minimum in the scattering rate $1/\tau$. The existence of the latter is presumably due to a corresponding minimum in the density of states, resulting from overlap effects across the faces of the Jones zone.[13] These overlap effects give rise to a maximum in the diamagnetic susceptibility of the γ_2 phase for the copper-aluminum system at exactly the same composition as the minimum in resistivity.[15] It is of interest that the resistivity of the δ-phase specimen appears to conform to the overall behavior of the γ_2-phase specimens, so that their electronic and transport properties must be very similar. Indeed, the present results are consistent with the conjecture that these phases are in fact not distinct.[3]

The present results for the bulk γ_2 and θ phases are similar to those obtained previously for thin-film specimens.[2] Therefore, the conclusions about the effects of annealing on the interfacial structure of thin-film copper-aluminum couples reported previously are not altered in any significant way.

ACKNOWLEDGMENTS

The authors would like to thank Dr. P. Coleridge for helpful discussions concerning dHvA measurements in dilute noble-metal alloys. This work was supported by the National Science Foundation, Materials Research Laboratory Section, under Grant No. DMR-8020246.

[1] J. A. Rayne, M. P. Shearer, and C. L. Bauer, Thin Solid Films 65, 381 (1980).
[2] C. Macchioni, J. A. Rayne, S. Sen, and C. L. Bauer, Thin Solid Films 81, 71 (1981).
[3] See, for example, W. B. Pearson, *Handbook of Lattice Spacings and Structures of Metals* (Pergamon, New York, 1958).
[4] J. O. Linde, Ph.D. thesis, Lund (1939) (unpublished).
[5] A. T. Robinson and J. E. Dorn, J. Metal. Trans. 3, 457 (1951).
[6] M. A. Biondi, and J. A. Rayne, Phys. Rev. 115, 1522 (1959).
[7] J. A. Rayne, Phys. Rev. 121, 456 (1961).
[8] F. d'Heurle, C. Alliota, J. Angilello, V. Brusic, J. Dempsey, and D. Irmischer, Vacuum 27, 321 (1977).
[9] See, for example, J. M. Ziman, *Principles of the Theory of Solids* (Cambridge University Press, Cambridge, 1972).
[10] E. A. Stern, Phys. Rev. 168, 730 (1968).
[11] P. T. Coleridge (private communication).
[12] L. Nordheim, Ann. Phys. (Leipzig) 9, 607 (1931); 9, 641 (1931).
[13] H. Jones, *Theory of Brillouin Zones and Electronic States in Crystals* (North-Holland, Amsterdam, 1960).
[14] B. W. Veal and J. A. Rayne, Phys. Rev. 132, 1617 (1963).
[15] C. Macchioni, K. R. Mountfield, and J. A. Rayne (unpublished).